PHYSICAL REVIEW B VOLUME 32, NUMBER 10 15 NOVEMBER 1985

Delocalization transition in random electrified chains with arbitrary potentials

Ernesto Cota* and Jorge V. José
Department of Physics, Northeastern University, Boston, Massachusetts 02115

M. Ya. Azbel
Tel Aviv University, 69978 Tel Aviv, Israel
(Received 17 June 1985)

This paper presents a study of the transmission properties of noninteracting electrons in the presence of different types of disordered potentials along a line, in a constant electric field F. We start by considering the case of random rectangular potentials. We use the transfer-matrix method to calculate numerically the transmission coefficient as a function of energy E, field F, length L of the sample, and the amount and type of disorder. An asymptotic analytic approach, based on different physical approximations, is shown to lead to good qualitative explanations of the numerical results. Armed with the analytic understanding of the numerical results as applied to the rectangular potential, we extend the logic to the cases of δ-function and continuous random potentials. We find that the results can be separated in two qualitatively different regimes. In the case where $X=FL/E<1$, the results for all different types of potentials considered are qualitatively the same, i.e., the states are localized and lead to *a linear correction in the resistance* as a function of the current. In the case when $X>1$, the situation is different: In the δ-function-potential case, and for small values of the field, the states remain localized but with a power-law decay for large L, as found previously. In the rectangular and smooth potential cases considered, we find a transition from localized to extended states as we vary the sample size L. The extended states are unusual in that they have a transmission coefficient which is nonlinear in F for large L. Possible consequences of these results to experiments with wires in metal-oxide-semiconductor field-effect transistors are also discussed.

I. INTRODUCTION

The nature of the spectrum of a noninteracting electron in a one-dimensional (1D) system in the presence of a random potential, at zero temperature, is by now well understood. The wave functions are exponentially localized and the spectrum is pure point and dense.[1-3] These results are mathematical and formal in nature. Landauer has given a way to relate these results to the measurable transport properties of experimentally realizable wires.[4,5] Landauer's approach is based on the scattering properties of an electron current incident on a disordered conductor. He finds a connection between the transmission properties of the scattering region and the resistance, which is now known as the Landauer formula,

$$R=T^{-1}-1\ . \tag{1.1}$$

In this equation, T represents the total transmission coefficient of the disordered scattering region and R is the dimensionless resistance. In a one-dimensional, one-channel model, at zero temperature, the resistance changes with the size of the system L as

$$R=e^{\alpha L}-1\ , \tag{1.2}$$

where α plays the role of an inverse localization length and is dependent on the type of potential variations inside the disordered region, and is independent of L. Several subtleties associated with the validity of Eq. (1.1) have been discussed in the literature.[6] Here we will not be concerned with those problems since they seem to have been settled to a large extent. Equation (1.2) reduces to the appropriate limits: When $\alpha \ll 1$, i.e., in the weak localization regime, one recovers Ohm's law, whereas for $\alpha \gg 1$, the strong localization case, one has the exponential increase in R as the system size increases.

The facts mentioned above are fairly well established by now. Less understood, however, are the effects of nonzero fields on the states of free electrons propagating in a random potential. Recently, several studies have begun to treat this problem when the external field is a constant electric field applied along the chain.[7-13] In all these studies, except Ref. 7, that considered a white noise potential, the model considered is a random-δ potential. There are several interesting results that have emerged from these studies, and one would like to know how potential dependent are these results.

The purpose of this paper is to extend the study of the effects of an electric field on the nature of the electronic states, when the potentials are random but not δ-function like. As we will show there are in fact important differences, mainly in the large-L limit, in which a transition between localized to extended states is achieved, even in the case of a small field.

With the intent of completeness, we will consider also the δ-function-potential case, to make comparisons to the results for all the other potentials studied in this paper. Our approach will be numerically exact for the case of a random symmetric rectangular potential. We develop an asymptotic analytic understanding of the results obtained in this case. We then proceed to consider the δ-function-

potential problem, in which the analytic approach is even quantitatively correct. Following the same logic as described above, we consider analytically the case of a smooth potential in the different limits of interest. Finally, we collect and compare the results obtained for the different random potentials studied. A previous mathematical analysis of a sufficiently smooth random potential problem in an electric field has been given in Ref. 14. There the authors show that in the infinite-volume limit all states are extended. Here we are interested in the length dependence of the scattering properties of these problems and their connection to their transport properties.

The outline of the paper is the following. In Sec. II we introduce the different potentials considered in the paper. In Sec. III the numerical analysis of the rectangular potential problem is presented. Here we replace the ramp potential produced by the electric field by a ladder potential. We show explicitly, however, that the results obtained by using an accurate algorithm to calculate Airy functions of large arguments lead to results which are of the same order of accuracy as the results obtained with the ladder potential, except that the latter are less computing intensive. In order to differentiate between results which depend on the periodic arrangement of the potentials, we consider two types of disorder. Randomness in the heights, and randomness in the positions with constant height and width for the potential. In Sec. III we give the results for the average transmission coefficient, together with its statistical properties, as a function of field, disorder, energy, and length of the sample, and type of randomness in the potential. In Sec. IV we present the bulk of our analytic results. For the rectangular and δ-function potential we make explicit comparison to the numerical results. In Sec. IV we extend the analytic treatment to a smooth random potential, where numerical results can be much more cumbersome. In Sec. V we discuss the consequences from the numerical and analytic results. In particular, we see that the problems divide clearly into two regimes in terms of the scale $X=FL/E$. When $X<1$, the states are localized. These localized states depend on F, and lead to a linear correction in F to the resistance. The coefficient of the correction term, although small in realistic samples, may be detectable experimentally. In the $X>1$ regime, the type of potential considered becomes important. We find important differences between the δ-function potential and potentials with a finite height. In the former case, for large L's the electronic states are power-law localized,[7,9,10] and therefore have zero conductance in the thermodynamic limit. In contrast, for the finite-height potentials for large L's, the electronic states are extended even for small F's. These extended states have, however, a nonlinear transmission coefficient as a function of F. Finally, we discuss briefly the possible connection of the results derived in this paper to experiments with wires in MOSFET's (metal-oxide-semiconductor field-effect transistors).

II. MODELS

In this section we define the models to be studied in this paper. We consider a system of noninteracting electrons, satisfying the time-independent Schrödinger equation,

$$\left[-\frac{d^2}{dx^2}+U(x)-Fx\right]\Psi=E\Psi\ . \tag{2.1}$$

Here E is the energy of the electron measured in atomic units, and Ψ is the wave function. The electrostatic potential is given by the $-Fx$ term in Eq. (2.1), with $F=\epsilon e$, e denoting the electronic charge, and ϵ the electric field strength. The potential $U(x)$ is random and has the general form

$$U(x)=\sum_{n=1}^{N} V_n(x-x_n)\ , \tag{2.2}$$

where $V_n(x-x_n)$ denotes the on-site potential with center at x_n, and N is the total number of potential barriers in a chain of length L. The bulk of our numerical results refer to a periodic array of rectangular on-site potentials separated by a fixed distance a, width fixed with b ($b<a$), and heights V_n (Fig. 1),

$$V_n(x-x_n)=\begin{cases}0, & |x-(n-1)a|\geqq b/2\ ,\\ V_n, & |x-(n-1)a|\leqq b/2\ .\end{cases} \tag{2.3}$$

The variables V_n are taken to obey a uniform probability law $P(V_n)=1/W$, and $C-W/2<V_n<C+W/2$, with C fixed.

In order to separate the effects that depend on the periodic nature of the lattice, from those which are only related to the effect of F, we also consider the case where V_n is the same for all n, but the locations of the potentials are random. We take $V_n(x-x_n)=V_0$, the width of the potential is fixed at b and the average separation between barriers is a. The location of the barriers is a random variable chosen as

$$x=(n-1)a+(s-0.5)W\ , \tag{2.4}$$

with s a uniformly distributed random number of width $W<b$, so that the rectangles do not overlap.

As we mentioned in the Introduction, apart from the models defined above, we study analytically a random δ-function potential and a continuous random potential. The δ-function potential is defined as

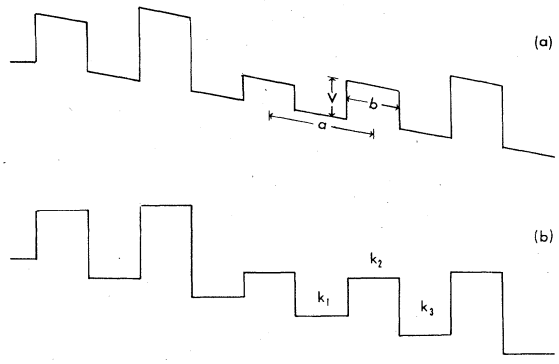

FIG. 1. Rectangular random potential in an electric field: (a) with a ramp $-Fx$ potential; (b) with its ladder approximation.

$$V_n=\beta_n\delta(x-na)\ , \tag{2.5}$$

with β_n a uniformly distributed random variable centered in zero and width W and a fixed. For this model we rederive the results reported in Refs. 9 and 10 even quantitatively. Finally, since the rectangular potential has a discontinuity in its first derivative, we also consider smooth potentials.

It is of interest to consider short-range smooth potentials V_n, clearly separated from each other. In this case a small E will only shift slightly the "wings" of the potential. With these types of potentials in mind we can write the transfer matrix for each potential explicitly. A typical example of a potential with these properties is

$$V_n=V_0/\cosh^2(x_n/\lambda)\ . \tag{2.6}$$

III. NUMERICAL TRANSFER MATRIX RESULTS FOR RECTANGULAR POTENTIALS

In this section we use the transfer-matrix (TM) method to calculate the ensemble averaged transmission coefficient for the rectangular models defined in the preceding section. The basic equation satisfied by the transfer matrix M reads

$$\Psi_r(x=L)=M\Psi_l(x=0)\ , \tag{3.1}$$

where Ψ_l is the wave function on the left of the disordered region and Ψ_r is its value on the right of the sample. The matrix M is a 2×2 matrix with elements that depend on the specific form of the potential. The matrix elements of M satisfy the identities, $M_{22}=M_{11}^*=M_{21}^*$. For the $-Fx$ potential, it is convenient to transform Eq. (2.1) using the change of variables

$$z=-F^{1/3}[x+(E-V)/F]\ , \tag{3.2}$$

leading to the standard Airy-equation representation,

$$\frac{d^2\Psi}{dz^2}+z\Psi=0\ . \tag{3.3}$$

The solution to this equation in the nth cell can be written in general as

$$\Psi_n=a_n\mathrm{Ai}(z)+b_n\mathrm{Bi}(z)\ . \tag{3.4}$$

Here the $\mathrm{Ai}(z)$ and $\mathrm{Bi}(z)$ are the Airy functions and (a_n,b_n) are constants. The construction of the transfer matrix is done by imposing the continuity of the wave function and its derivative at the points of discontinuity of the potential. Explicitly, for a given potential barrier, as shown in Fig. 1, one gets

$$M(na)=T^{-1}(na+b/2)S(na+b/2)\times S^{-1}(na-b/2)T(na-b/2)\ , \tag{3.5}$$

with

$$T(z)=\begin{bmatrix}F(z) & G(z)\\ F'(z) & G'(z)\end{bmatrix}\ , \tag{3.6}$$

and

$$S(z)=\begin{bmatrix}f(z) & g(z)\\ f'(z) & g'(z)\end{bmatrix}\ , \tag{3.7}$$

where the prime stands for differentiation with respect to x. Here, (F,f) are Ai functions and (G,g) are Bi functions. See Ref. 15 for the definition of these functions. For a chain of length L with N potential barriers in between, M reads

$$M=\prod_{i=1}^{n}m(ia)\ . \tag{3.8}$$

In the numerical evaluation of M we need to generate Airy functions of large argument with precision. There is a very accurate algorithm to generate the Airy's of arbitrary argument based on Chebyshev's series approximation.[16] We use that method in our calculations.

An equivalent way to represent the effect of the electrostatic potential is to replace the $U(x)-Fx$ potential by a ladder (Fig. 2). Specifically, we write the potential as

$$U(x)-Fx=\begin{cases}V_n-F(n-1)a, & 0\leq x-(n-1)a\leq b\\ -F(n-1)a, & \text{otherwise}\ .\end{cases} \tag{3.9}$$

The advantage of taking this potential instead of the $U(x)-Fx$ potential is that in the former case the transfer matrix takes the following, relatively simpler form (see Fig. 3 for the definition of the cell potential),

$$M_{11}=\frac{k_1}{4k_3}(\alpha_{21}\alpha_{32}e^{ik_2b}+\alpha'_{21}\alpha'_{32}e^{-ik_2b})e^{i(k_{13}na-k'_{13}b/2)}\ , \tag{3.10}$$

$$M_{12}=\frac{-k_1}{4k_3}(\alpha'_{21}\alpha_{32}e^{ik_2b}+\alpha_{21}\alpha'_{32}e^{-ik_2b})e^{i(k_{13}na-k'_{13}b/2)}\ . \tag{3.11}$$

Here we defined $\alpha_{21}=1+k_2/k_1$, $\alpha_{32}=1+k_3/k_2$,

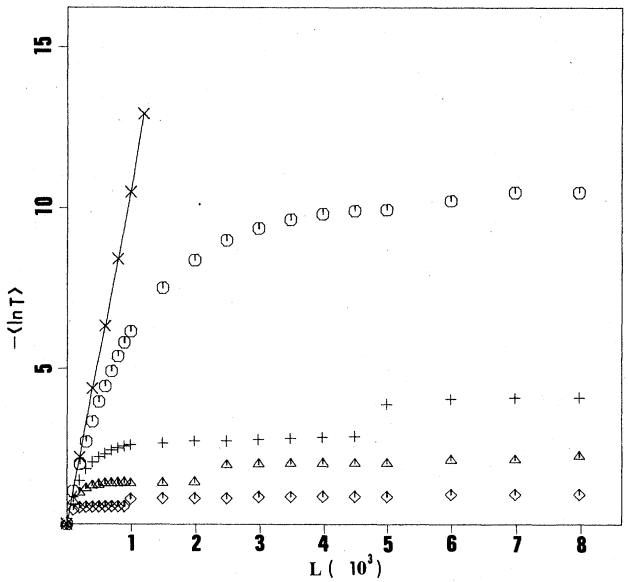

FIG. 2. Ensemble averaged $\ln T$ vs L for different values of the field F. ×, $F=0$; ⊙, $F=0.001$; +, $F=0.004$; △, $F=0.008$; ◇, $F=0.02$. Here we took $E=4$, $C=1$, and $W=2$.

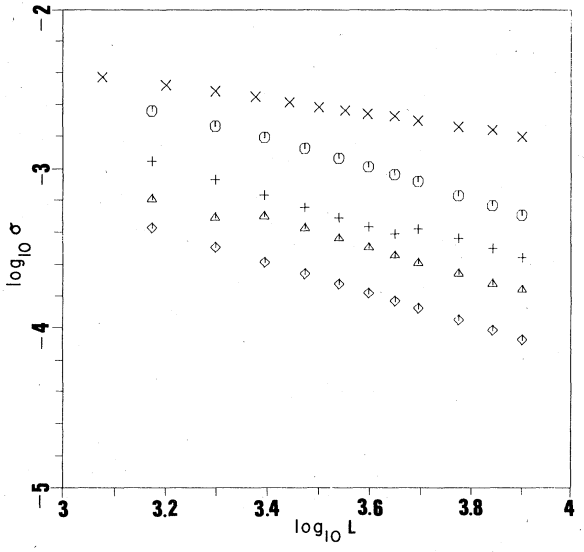

FIG. 3. $\log\sigma$ vs $\log L$ with the same parameter values as in Fig. 2.

TABLE I. Comparisons of the results for $-\langle \ln T\rangle$ of the ramp potential, in terms of Airy functions, and that of the ladder potential for the parameter values given in the table, with $E=4$, $C=1$, and $W=2$.

	$F=0.008$	
L	Ladder approximation	Exact (Airy functions)
1000	0.001 271 44	0.001 241 41
2000	0.000 660 13	0.000 644 35
3000	0.000 627 40	0.000 609 57
4000	0.000 474 92	0.000 462 13
5000	0.000 380 78	0.000 370 25
	$F=0.5$	
L	Ladder approximation	Exact (Airy functions)
1000	0.000 064 51	0.000 092 98
2000	0.000 032 66	0.000 047 13
3000	0.000 022 37	0.000 031 63
4000	0.000 016 86	0.000 023 46
5000	0.000 136 7	0.000 018 74

$\alpha'_{21}=1-k_2/k_1$, $\alpha'_{32}=1-k_3/k_2$, $k_{13}=k_1+k_3$, and $k'_{13}=k_1-k_3$. The k's represent the momentum in the mth cell and in the case shown in Fig. 3 they are given by

$$k_1=[E+F(na-b/2)]^{1/2},$$
$$k_2=[E-Vn+F(na-b/2)]^{1/2}, \tag{3.12}$$
$$k_3=[E+F(na+b/2)]^{1/2}.$$

Calculating M in this case entails evaluations of plane-wave–like functions and is therefore more efficient computationally. The results from using either the ramp or ladder representation compare quite well. In Table I, we give some results obtained with both potentials for two values of F. For small values of F we see that the results differ only in the fifth significant figure. The difference is of the same order but more significant for larger values of F as expected. Thus the results presented below were obtained using the ladder potential and transfer matrices given in Eqs. (3.11) and (3.10).

We obtain the transmission coefficient T from the expression

$$T=k_0/(k_r|M_{11}|^2), \tag{3.13}$$

with $k_0=\sqrt{E}$, the momentum of the incident electronic wave, and $k_r=\sqrt{E+FL}$, that of the emerging wave. We are interested in calculating ensemble-averaged quantities. As in the $F=0$ case we calculate the ensemble average of $-\ln T$. As usual, we generate an ensemble of chains for a given length and average the natural log of their transmission coefficients. To check that this is indeed the right statistical variable in this problem, in Fig. 4 we show a plot of $\ln\sigma$ versus $\ln L$, where σ is the standard deviation of $-(\ln T)/L$, defined as

$$\left[\frac{\langle(\ln T-\langle\ln T\rangle)^2\rangle}{L^2}\right]^{1/2}.$$

In the case $F=0$, we get a straight line with slope close to $-\frac{1}{2}$, as expected from the standard central-limit theorem. When $F\neq 0$, on the other hand, we get a straight line but the slope is larger the larger F is.

In Fig. 2 we show the results for $-\langle \ln T\rangle$ versus L for a fixed value of the disorder and energy, and different values of the field. First, as expected, we see that for $F=0$ the curve is a straight line indicating exponential localization. When $F\neq 0$, on the other hand, we notice two types of behavior. For small L's the $-\langle \ln T\rangle$-versus-L curve is close to a straight line. However, for larger L's

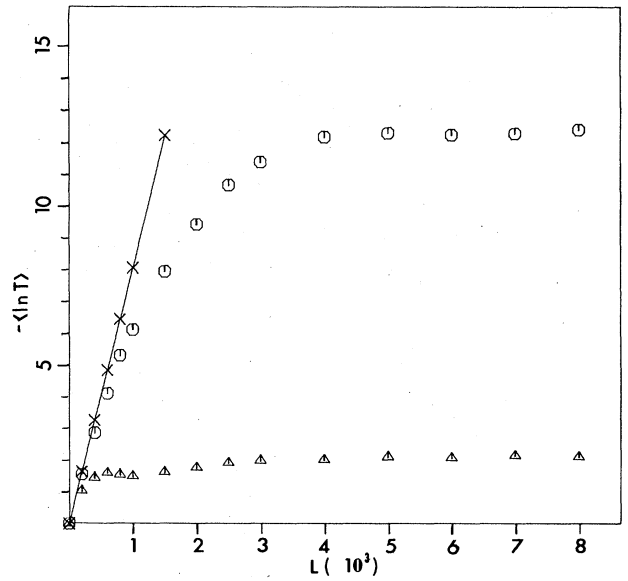

FIG. 4. Same as in Fig. 2 for the case where the rectangular potentials are randomly located with fixed shape. Here we took $E=4$ and $W=1$, and ⊙, $F=0.001$; △, $F=0.008$.

the curve saturates to essentially a constant value. The points at which the curves change from straight to flat is for $X=FL/E$ of order unity. This is easy to understand physically. For $X \ll 1$, the kinetic energy gained by the electron from the field is small compared to its incoming energy and, therefore, the random potential is dominant. When $X \gg 1$ the electron gains sufficient kinetic energy from the field that the potential becomes a small perturbation. For this reason, X is the important scale in these problems. Notice in Fig. 2 that the value of saturation for $-\langle \ln T \rangle$ for large L's changes considerably for relatively small changes in F. Also, we see from Figs. 2 and 3 that the curves have a noticeable jump for values of $X \approx 4$. We believe that this is due to the periodic nature of the potential. To test that this is indeed the case, we show in Figs. 4 and 5 the results obtained when using the rectangular potential with random locations. There is no noticeable jump in these curves and therefore the abrupt changes seen in Figs. 2 and 3 should be related to the periodic lattice structure of the random potentials. The jump may be either related to Zener tunneling or due to the special "delocalization" points that can be found in the spectrum.[17]

From the $F=0$ calculation we can extract the localization length l_c, as the inverse of the slope of the straight line. Using this value for l_c we can plot $-l_c\langle \ln T \rangle/2L$ versus X. The resulting plot is shown in Fig. 6. In this figure we show results for different values of F and W for a fixed value of E. The choice of parameters was made carefully such that the energy was not in a gap of a given potential distribution. We see that all the results change in qualitatively the same way. These curves are the analog of the universal curve found in the δ-function-potential case.[9] We find different curves here because we are essentially comparing random potentials with different average heights. In the next section we will derive analytically the curve that fits qualitatively our numerical

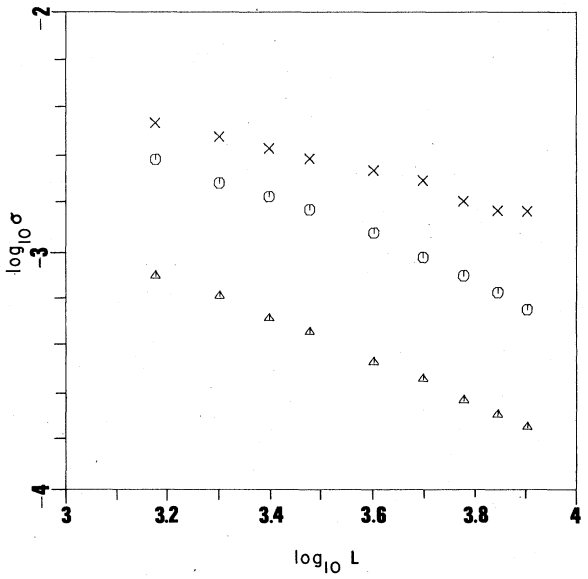

FIG. 5. Same as in Fig. 3 for the same system and parameter values of Fig. 4.

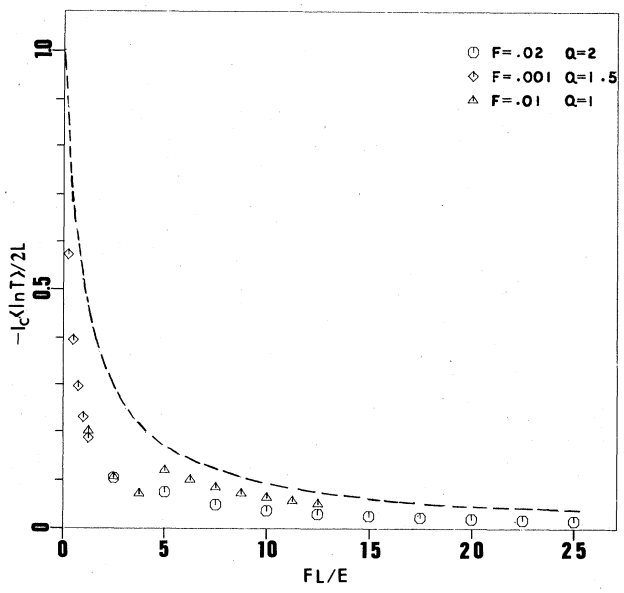

FIG. 6. Plot of different calculations of $-(l_c \ln T)/2L$ vs $X=FL/E$ for the parameters shown in the inset. The discontinuous line corresponds to the theoretical result $1/(X+1)$.

results and is shown as a broken line in Fig. 6.

Notice that, apart from the jump due to Zener tunneling, there is no abrupt change in the $-\langle \ln T \rangle$-versus-L curves when going from localized to extended states. We will discuss in more detail the results given above in terms of the analytic treatment given next.

IV. ANALYTIC, ASYMPTOTIC, HEURISTIC APPROACH

In this section we give a heuristic explanation of our numerical results pertaining to the rectangular random potentials.[17] We extend our analytic treatment to treat also the δ-function-potential case and find even quantitative agreement with the numerical results given in Ref. 9. Finally, we consider the potential defined in Eq. (2.6) using the same methods and obtain explicit expressions for the averaged transmission coefficient in the small- and large-X regimes.

A. Rectangular potential

To calculate the average transmission coefficient of a periodic array of random-height rectangular potential barriers, we will consider the following two different physical cases: When the energy of the wave is below the height of the first potential barrier, and when it is above the highest of the potential barriers in the chain. In the first case the wave will be strongly reflected, and the transmission coefficient will be small. If E is smaller than the mean height of the potential barriers, we can calculate the net transmission coefficient of the set of barriers for which the above condition is satisfied as

$$T=\prod_n t_n \ , \tag{4.1}$$

where t_n is the transmission coefficient of the nth barrier. In this equation we have neglected the effect of multiple reflections. We can calculate the value of t_n by using the WKB approximation, leading to

$$T=\prod_n \exp\{-2b[\langle V_n\rangle-(E+Fn)]^{1/2}\}$$
$$=\exp\left[-b\int_0^L[\langle V_0\rangle-(E+Fx)]^{1/2}dx\right]. \quad (4.2)$$

Here we are neglecting logarithmic corrections in the exponent that would come from an evaluation of the coefficient in front of the exponential. We have also changed the sum over n by an integral over x, since we are considering many potentials and the $-Fx$ potential changes slowly. Also we have taken for the potential barrier height the mean value of $\langle V_n\rangle$. After carrying out the integration we can write $-\ln T$ as

$$-\ln T=\frac{4}{3}\frac{b}{F}(\Delta E)^{3/2}\left[1-\left[1-\frac{FL}{\Delta E}\right]^{3/2}\right], \quad (4.3)$$

where we defined $\Delta E=V_0-E$. We notice that in the $F=0$ limit we recover the result of exponential localization, with localization length

$$l_c^{-1}=b(\Delta E)^{1/2}. \quad (4.4)$$

The next order contributions to $-\ln T$ can be calculated directly from Eq. (4.3) obtaining

$$-\ln T\cong\frac{2L}{l_c}\left[1+\frac{1}{4}\frac{FL}{\Delta E}\right]. \quad (4.5)$$

As long as the total energy of the electron does not exceed the maximum height of the potential barriers the results described above will hold. This will be true particularly for very small F's and not overly large L's.

Since the wave continuously gains energy as it travels along the chain, eventually a crossover from E below to E above the barrier takes place. In the last case, the reflection coefficient r_n is small and we can write

$$T\cong\prod_{n=1}^{n}(1-r_n)=\exp\left[-\sum_n r_n\right]. \quad (4.6)$$

This result is again obtained within the approximation of neglecting multiple reflections. We can estimate the value of r_n easily from the exact calculation of the transmission coefficient for a rectangular barrier or from the WKB approximation for reflection above a barrier.[18] The result for T becomes

$$T=\exp\left[-\sum_n\frac{1}{8}\frac{\langle V_0^2\rangle}{(E+Fn)^2}\right]$$
$$=\exp\left[-\int_0^L\frac{1}{8}\frac{\langle V_0^2\rangle}{(E+Fx)^2}dx\right], \quad (4.7)$$

which leads to

$$-\ln T=\frac{\langle V_0^2\rangle}{8E^2}L\left[1+\frac{FL}{E}\right]^{-1}. \quad (4.8)$$

We can define a localization length in this case for the $F=0$ limit, which is

$$l_c^{-1}=\frac{\langle V_0^2\rangle}{16E^2}. \quad (4.9)$$

For the calculations presented in the previous section with $E=4$, $W=2$, and $C=1$ we see that $l_c=194.932$, whereas the analytic result gives $l_c=191.554$. This result is quite good taking into account the approximations made.

We return to Eq. (4.8) when $F\neq 0$. For X small we can expand $-\ln T$, giving,

$$-\ln T=\frac{2L}{l_c}[1-X+X^2+O(X^3)]. \quad (4.10)$$

This is an important result since we see that the leading correction to the standard exponential decay of T with L is linear in F, and in turn it leads to a linear correction in the resistance [Eq. (2.2)]. We shall discuss this point further in the next section. When X is large, $-\ln T$ becomes

$$-\ln T=\frac{2E}{l_cF}[1-X^{-1}+X^{-2}+O(X^{-3})]. \quad (4.11)$$

Thus, as L tends to infinity, $-\ln T$ reaches a constant value. Equivalently, the states tend to become extended. These extended states are not of the same type one finds in a periodic solid since T is a highly nonlinear function of F with an essential singularity for $F=0$. This result also agrees with our numerical results. This can be seen from looking at Figs. 2 and 4, which are qualitatively described by the result given in Eq. (4.8).

In order to carry out quantitative comparisons we have to be in the very large L limit, or equivalently large X regime. We see that the heuristic analysis gives qualitatively the correct behavior of $-\ln T$ in the asymptotic limits of $X\ll 1$ or $X\gg 1$ and we connect these two regimes with the numerical results.

For a potential that has other types of discontinuities in its derivatives, as for example $V\sim(x-x_0)^\nu$ for some x_0 along the chain, and that leads to $r\sim 1/E^\nu$ for E's above the height of the barrier and with $\nu\geqq 2$, the analysis given above yields

$$-\ln T=\frac{C_\nu}{E^\nu}L[1-\tfrac{1}{2}\nu X+O(X^2)], \quad (4.12)$$

for $X\ll 1$. Here C_ν is a constant that depends on the potential and the mean of its random fluctuations. In the $X\gg 1$ limit we get

$$-\ln T=\frac{C_\nu}{E^{\nu-1}F^{(\nu-1)}}[1-X^{-\nu+1}+(\nu-1)X^{-\nu}+\cdots]. \quad (4.13)$$

The results written above reduce, as they should, to the rectangular case results for $\nu=2$, and are qualitatively equivalent to them. Notice that ν is not necessarily an integer (in fact, ν is related to the nature of the reflection point in the complex phase plane of the WKB analysis), and thus Eqs. (4.12) and (4.13) imply a continuum variation of T as a function of the "critical exponent" ν.

B. δ-function potential

As we mentioned in the Introduction, most of the studies of electronic states in electrified chains have been carried out assuming a distribution of random-δ-function potentials. Here we reconsider this problem for completeness, following the line of thought used in Sec. IV A. The model is defined by Eqs. (2.1), (2.2), and (2.5). The transmission coefficient of a single δ-function potential is

$$t=(1+\beta^2/4E)^{-1} .$$

In this case, the analogue of barrier height is the strength of the potential β. Therefore, the limits $\beta^2>E$ and $\beta^2<E$ correspond to "above" and "below" the barrier. Since for $F\neq 0$, E goes to $E+Fx$, the case of interest corresponds to E above the "barrier." In this limit, the reflection coefficient $r\sim 1/E$, and the total transmission coefficient for a chain of length L can be approximated by

$$T\sim\prod_{n=1}^{N}(1-r_n)\sim\exp\left[-\int_0^L\frac{\langle\beta^2\rangle}{4(E+Fx)}dx\right]$$
$$=\exp\left[\frac{-\langle\beta^2\rangle}{4F}\ln(1+x)\right] . \quad (4.14)$$

In the limit $X=0$, we recover the exponential localization result,

$$T=\exp\left[-\frac{\langle\beta^2\rangle}{4E}L\right] . \quad (4.15)$$

It is interesting to notice that if we take β uniformly distributed between $-W/2$ and $W/2$, we obtain the localization length

$$l_c=\frac{96E}{W^2} , \quad (4.16)$$

which is exactly the same result as the one obtained by a more detailed analytic study.[19] The next-order corrections to T as a function of X gives

$$-\ln T=\frac{2L}{l_c}[1-X/2+X^2/3+O(X^3)] . \quad (4.17)$$

As shown in Ref. 9, this result leads to a linear correction in F to the resistance. We shall discuss this result further in the next section. In the limit where $X>1$ we get from Eq. (4.14),

$$T=(F/E)^{-\langle\beta^2\rangle/4F}L^{-\langle\beta^2\rangle/4F} . \quad (4.18)$$

This is the power-law localization result confirmed numerically and theoretically in Ref. 9. The consequences from this result are given in Ref. 9, and we will compare them to the results obtained for other potentials in the next section.

C. Continuous potential

The results given in Secs. II A and II B apply to potentials that have different types of discontinuities. It is natural to ask if the results should change significantly if the potentials are smooth rather than discontinuous. Numerical calculations for smooth potentials are much more cumbersome to perform. On the other hand, we can follow the same logic as expounded in this section to get results that should be valid asymptotically. Here we consider the potential given in Eq. (2.6) explicitly, but the results for other continuous potentials clearly separated from each other are qualitatively the same. We will use the WKB method to calculate the reflection and transmission coefficients for a wave with energy E above and below the barrier. For $E<\langle V_0\rangle$, the transmission coefficient is given by[20]

$$t\sim\exp[-2\pi\lambda(V_0^{1/2}-E^{1/2})] , \quad (4.19)$$

where we have taken the limit $1<\lambda$. Given the approximation of Eq. (4.1), we get for T the expression

$$-\ln T=2\pi\lambda\left\{V_0^{1/2}L+\frac{2}{3}\frac{E^{3/2}}{F}\left[1-\left[1+\frac{FL}{E}\right]^{3/2}\right]\right\} . \quad (4.20)$$

In the limit where $X\ll 1$, this result reduces to

$$-\ln T=2\pi\lambda(V_0^{1/2}-E^{1/2})L\left[1-\frac{1}{4}\frac{FL}{E}\left[\frac{E^{1/2}}{V_0^{1/2}-E^{1/2}}\right]\right] , \quad (4.21)$$

again of the same form as the results obtained in Eqs. (4.10), (4.15), and (4.16). In the important limit where the energy E is far above V_0, using the WKB approximation one gets the reflection coefficient[18]

$$r\sim e^{-2\pi\lambda\sqrt{E}} . \quad (4.22)$$

Using the approximation given in Eq. (4.12), we get for T

$$-\ln T=Le^{-2\pi\lambda\sqrt{E}}[1-\tfrac{1}{4}(4\pi\lambda\sqrt{E}+1)X+O(X^2)] , \quad (4.23)$$

good to lowest order in X, and

$$-\ln T\cong\left|[(2\pi\lambda\sqrt{E}+1)/2\pi^2\lambda^2F]e^{-2\pi\lambda\sqrt{E}}-\left[\frac{L}{F}\right]^{1/2}\frac{1}{\lambda\pi}e^{-2\pi\lambda\sqrt{FL}}\right| , \quad (4.24)$$

for $X\gg 1$. In the $X\ll 1$ limit we see, once more, that the general structure of the result is the same as for all the other potentials considered in this paper, thus one could conclude that the behavior of T for small X is in fact generic. In the $X\gg 1$ limit, we notice from Eq. (4.24) that in the limit of large L's, T tends to a constant value which is nonlinear in $1/F$. The approach to the $L=\infty$ limit is, however, exponentially faster than in the case where the potentials are discontinuous. The general characteristics of the results for the potential given in Eq. (2.6) will prevail for other types of smooth potentials for which $r\sim e^{-cE^{\nu}}$. An example of other types of smooth potentials for which this is true is $V(x)=V_0\exp(-x^2/\lambda^2)$, where $\nu=1$.

From all the results derived in this section we can conclude that the transmission coefficient, in the limit of

small X's, behaves in qualitatively the same way for all possible types of potentials. In contrast, for $X \gg 1$ there is a clear difference between the δ-function potential and any other potential with finite heights. The possible experimental consequences of the results described above will be given next.

V. CONCLUSIONS AND POSSIBLE EXPERIMENTAL CONSEQUENCES OF THE RESULTS

In this section we express the results obtained in the previous sections in terms of the conductivity properties of a random chain in an electric field, for different random potentials. As we have learned, the important scales in this problem are the localization length and $X = FL/E$.[21] In the limit of small X we can use the Landauer formula (2.1) to obtain the corrections to the resistance due to the presence of a nonzero F. For all the potentials considered here in the limit when $X \ll 1$ the resistance can be written as

$$\frac{\Delta R}{R_0} = \alpha_1 \frac{|V|}{E} - \alpha_2 \frac{|V|^2}{E^2} + \cdots , \tag{5.1}$$

where α_1 and α_2 are dimensionless constants and $V = FL$ is the potential energy difference between the ends of the sample. The values of the constants depend on the form of the potential and were given in the preceding section. Thus, we conclude that the effect of F in a random chain, in the limit of small X's, is qualitatively the same for all the potentials considered here. It leads to a linear correction in $|V|$ which is different from the usual Joule heating correction which goes as V^2. This result was obtained in Ref. 9, for the δ potential, and it is shown here that it is qualitatively the same for other types of potentials. Since the V^2 correction is obtained from considerations of analyticity of R as a function of V, one is led to conclude that even in the small-X limit the expansion in powers of V is nonanalytic.

The difference in the results arises in the regime $X \gg 1$. In this limit, we showed that in the discontinuous potentials as well as in the smooth potential cases, there is a transition to quasi-extended states for large L's with the rather unusual characteristic of having a transmission coefficient that is exponential in $-1/F$. In this limit, the electrostatic field dominates the effects of the random potential, and since the height of the potentials is finite, as the waves gain more and more kinetic energy they essentially behave as free particles in a ramp potential. The δ-function-potential case is different in that the potential reflects at all energies since the height is essentially infinite. A connection between this result for T in terms of the resistance cannot be given in terms of the Landauer formula since this is believed to be true in the limit of small F's.

In this paper we have considered the effect of an arbitrary electric field on the nature of the electronic states in a chain with arbitrary random potentials. It is possible that some of the predictions made here can be seen experimentally, especially the linear correction in $|V|$ of the nonlinear resistance. Our calculations have considered a free-electron model, as in most localization studies, in the presence of a constant electric field. We have left out two rather important physical effects in our analysis. The effects of temperature and the Coulomb interaction between electrons that lead to screening. It is not clear how to include these effects at the same level of rigor of the numerical results presented here.

Physically, at finite T's, the kinetic energy gained by the electron due to the field is FL, with L replaced by either l_{in} (inelastic mean free path) or $l_T = (l_{\text{in}} l_{el})^{1/2}$ (the Thouless length). After the electron travels a distance L it loses its energy to the phonons, and its energy goes back to the value of the electrostatic potential at distance x along the chain. The process is repeated again for distance $x + L$, etc.

If we take E as the Fermi energy of the electrons we see that the correction term on Eq. (5.1) is rather small in metals but not so small in semiconductors, since E_F is several orders of magnitude smaller in semiconductors than in metals. Experiments in MOSFET's (Refs. 22 and 23) may be appropriate to see the effects described in this paper. In those experiments it is found that the conductance is a rapidly varying function of gate voltage or, equivalently, E. The behavior of the maxima in the conductance as a function of temperature is found to follow the Mott law $\sim \exp -(T_0/T)^{1/2}$. This is typical of variable range hopping with $T_0 \sim 1/l_{\text{loc}}(E)$, where l_{loc} is the localization length. The experimental results as a function of E are fitted with a function $T_0 \sim e^{-aE}$. This behavior may be accounted for by the result given in Eq. (4.23), and therefore implies that the appropriate models to describe these experiments are the continuous potentials studied in Sec. IV. At finite T, the quantity $y = FL/k_B T$, with k_B Boltzmann's constant, becomes the relevant scale in the problem. In the large-y limit the results given in Eq. (4.24) may be seen in the 1D MOSFET's, in the millidegree temperature range, particularly in, the strong nonlinear behavior of the conductance with F.

ACKNOWLEDGMENTS

One of us (E.C.) wants to acknowledge the financial support from Consejo Nacional de Ciencia y Tecnologia (Mexico), The National University of Mexico, and the American Physical Society. The work done at Northeastern University was partially supported by National Science Foundation under Grant No. DMR-85-00531. We thank J. F. Reyes for calling Ref. 16 to our attention and A. Widom for informative discussions.

*Permanent address: Laboratorio de Ensenada, Instituto de Fisica, Universidad Nacional Autónoma de México, Apartado Postal 2681, Ensenada, Baja California, Mexico.

[1]N. F. Mott and W. T. Twose, Adv. Phys. **10**, 107 (1960).

[2]K. Ishii, Prog. Theor. Phys. Suppl. **53**, 77 (1973); R. Herendon and P. Erdos, Adv. Phys. **31**, 65 (1982).

[3]H. Kunz and B. Soulliard, Commun. Math. Phys. **78**, 201 (1980).

[4]R. Landauer, Philos. Mag. **21**, 863 (1970). A more general formula is derived in M. Ya. Azbel, Solid State Commun. **45**, 527 (1983).

[5]P. W. Anderson, D. J. Thouless, E. Abrahams, and D. Fisher, Phys. Rev. B **22**, 3519 (1980).

[6]D. J. Thouless, Phys. Rev. Lett. **47**, 972 (1981).

[7]V. N. Prigodin, Zh. Eksp. Teor. Fiz. **79**, 2338 (1980) [Sov. Phys.—JETP **52**, 1185 (1980)].

[8]J. Flores, J. V. José, and G. Monsivais, J. Phys. C **16**, L103 (1983).

[9]C. M. Soukoulis, J. V. José, E. N. Economou, and P. Sheng, Phys. Rev. Lett. **50**, 764 (1983).

[10]F. Delyon, B. Simon, and B. Soulliard, Phys. Rev. Lett. **52**, 2187 (1984).

[11]J. V. José, G. Monsivais, and J. Flores, Phys. Rev. B **31**, 6906 (1985).

[12]F. Bentosela, V. Grecchi, and F. Zironi, Phys. Rev. B **31**, 6909 (1985).

[13]E. Cota, J. V. José, and G. Monsivais (unpublished).

[14]F. Bentosela *et al.*, Commun. Math. Phys. **88**, 387 (1983).

[15]*Handbook of Mathematical Functions,* edited by M. Abramowitz and I. Stegun (Dover, New York, 1968).

[16]P. J. Prince, ACM Trans. Math. Software **1**, 372 (1975).

[17]M. Ya. Azbel, Phys. Rev. B **28**, 4106 (1983).

[18]V. L. Pokrovskii *et al.*, Zh. Eksp. Teor. Fiz. **34**, 1272 (1953); **34**, 1629A (1953) [Sov. Phys.—JETP **34**, 879 (1953); **34**, 1119 (1953)]; see also M. V. Berry, J. Phys. A **15**, 3693 (1982); M. V. Berry and K. E. Mount, Rep. Prog. Phys. **35**, 315 (1972).

[19]M. Kappus and F. Wegner, Z. Phys. B **45**, 15 (1981).

[20]L. D. Landau and E. M. Lifschitz, *Quantum Mechanics,* 3rd ed. (Pergamon, New York, 1977).

[21]We have used atomic units in our calculations. The unit of length is the Bohr radius $a=5.29\times10^{-11}$ m. The atomic unit of electric field gives the factor $f=2.571\times10^{9}$ V/cm, thus F becomes Ff. The unit of energy is equal to 13.6 eV. Thus we can convert our parameter values to those in the laboratory by using the conversion factors given above.

[22]A. B. Fowler, A. Hartstein, and R. Webb, Phys. Rev. Lett. **48**, 196 (1982); R. G. Wheeler, K. K. Choi, A. Goel, R. Wisnieff, and D. Prober, *ibid.* **49**, 1674 (1982); R. F. Kwasnick, M. A. Kastner, J. Melngailis, and P. Lee, *ibid.* **52**, 224 (1984).

[23]A. Hartstein, R. A. Webb, A. B. Fowler, and J. J. Wainer, Surf. Sci. **142**, 1 (1984); R. Webb, A. Hartstein, J. J. Weiner, and A. B. Fowler, Phys. Rev. Lett. **54**, 1577 (1985).